Modified Instantaneous Power Control with Phase Compensation and Current-limited Function under Unbalanced Grid Faults

Liu, Wenzhao; Blaabjerg, Frede; Zhou, Dao; Chou, Shih-Feng

Published in:
IEEE Journal of Emerging and Selected Topics in Power Electronics

DOI (link to publication from Publisher):
10.1109/JESTPE.2020.2984475

Publication date:
2021

Document Version
Accepted author manuscript, peer reviewed version

Modified Instantaneous Power Control with Phase Compensation and Current-limited Function under Unbalanced Grid Faults

Wenzhao Liu, *Member*, *IEEE*, Frede Blaabjerg, *Fellow*, *IEEE*, Dao Zhou, *Senior Member*, *IEEE* and Shih-Feng Chou *Member*, *IEEE*

***Abstract*—In distributed generation systems, power quality is one of the main concerns during short-term unbalanced grid voltage faults. However, for the most common three-phase three-wire grid-connected inverters based power systems, there may be a trade-off between power oscillations and current harmonics during the unbalanced grid fault ride through control, which has a crucial impact on the installed inverters for different applications. In this paper, a modified instantaneous power control based voltage phase compensation control strategy is proposed to enhance the inverter current quality, while at the same time mitigating the active/reactive instantaneous power oscillations. Moreover, a simplified peak current-limited control strategy is developed to improve the reliability of the grid-connected system, and it does not need the extraction of the grid voltage and/or current fundamental positive/negative sequence components, which significantly reduce the computation burden. Finally, the experimental tests based on dSPACE-DS1007 and MATLAB/Simulink are carried out to verify the effectiveness of the proposed strategy.**

Index Terms— power quality, inverter, unbalanced grid voltage fault, reliability

I. INTRODUCTION

Distributed generation systems integrated with renewable energy resources (RES) are attracting more and more attention around the world [1-3]. With the development of a high penetration of RESs, more power electronic grid-connected inverters, which act as the interfaces between RESs and grid, should have the ability to improve the power quality and ride through the grid short-term faults or potential disturbances, especially under unbalanced grid voltage conditions[4]. More specifically, the grid codes require the grid-connected inverters not only to remain connected to ride through the grid short-term faults, but also to support the grid voltage recovery, generate profits, and eliminate the voltage unbalances with a certain amount of active/reactive power injections, also known as Fault Ride Through (FRT) ability [5]. Under these requirements, many interesting FRT control solutions have been presented based on instantaneous power theory [6-8].

Manuscript received December 10, 2019; revised February 26, 2020; accepted March 23, 2020. This work was supported by the VELUX FOUNDATIONS under the VILLUM Investigator Grant Reliable Power Electronic-Based Power System (REPEPS) (Award Ref. No.: 00016591) (Corresponding author: Dao Zhou)

Wenzhao Liu, Frede Blaabjerg, Dao Zhou and Shih-Feng Chou are with the Department of Energy Technology, Aalborg University, Aalborg 9220, Denmark (e-mail: wzl@et.aau.dk, fbl@et.aau.dk, zda@et.aau.dk, and shc@et.aau.dk)

In general, FRT control algorithms that are mainly based on symmetric positive and negative sequences to achieve particular control objectives such as the current harmonics, power oscillations, dc bus ripples, voltage support and over current limitation with different voltage/current references during the unbalanced grid faults have been proposed in [9], [10]. A significant contribution made by P. Rodriguez et al is the flexible power control concept in 2007 [11], and later several interesting FRT strategies focusing on the flexible power quality regulation are presented. As an example, the output current harmonics can be eliminated at the expense of active/reactive power oscillations [12]. The flexible pliant active and reactive power control is presented to improve the power quality of installed inverters during unbalanced grid voltage dips [13]. Another FRT solution is flexible since the positive and negative, active and reactive power/current can be simultaneously injected into the grid to improve the stability and reliability of ride through services of grid-connected inverters [14].

On the other hand, the instantaneous power theory has recently been applied to control of single-phase and three-phase grid-connected inverters [15-18]. More analysis and design of active and reactive power control for operating inverters in a flexible way during unbalanced grid faults can be found in [19-21]. However, for the three-phase three-wire grid-connected inverter system, the control freedoms may not be enough to eliminate instantaneous power oscillations and current harmonics at the same time due to clear lack of the path for zero sequence voltage/current components [22]. Therefore, some three-phase four-wire systems were introduced to enhance the controllability and flexibility of inverters [23-25]. However, these three-phase four-wire systems are designed for special devices and need more complex control structure, which is not convenient for further applications.

Furthermore, some direct power control methods have recently been proposed for inverters without any inner-loop current regulators [26], [27]. However, these methods need variable switching frequency based on different switching states, and will cause more harmonics and need more complex design of the line filters. A grid voltage modulated direct power control method was reported in [28] and it has a good transient response and steady-state performance. However, the method has not considered the impact of actual three-phase overcurrent and harmonics. In fact, the excessive and harmonic current significantly affects the stability and reliability of the grid-connected power system, and the instantaneous power oscillations will damage the

This article has been accepted for publication in a future issue of this journal, but has not been fully edited. Content may change prior to final publication. Citation information: DOI 10.1109/JESTPE.2020.2984475, IEEE Journal of Emerging and Selected Topics in Power Electronics

continuity of power supply at both dc link and ac side, especially during the unbalanced grid faults [29].

As described in [30-32], there are several methods to provide current limitation and stability for grid-connected inverters under unbalanced grid faults. In [33], the inverter switches its control structure to a hysteresis control if the permissible current is exceeded. In a similar way, a grid-following mode control method during unbalanced grid fault is proposed in [34], but it needs extra PLLs for the grid synchronization. On the other hand, the current limitation can be achieved by simply controlling the current references within a range of limited value, but may cause instability and lead to a wind-up in power control loops. [35]. As one solution, the virtual impedance structure for current limitation is proposed in [36], but the method needs the detection of the fault location, and the selection of virtual impedance are quite complex for further applications [37], [38].

In fact, very few works have been developed for both power quality control and peak current-limited capacity for grid-connected inverter under unbalanced and extremely weak grid faults. On one hand, in contrast to conventional reactive power theory, the active and reactive power should be estimated accurately while at same time the output current harmonics should be reduced to improve the power quality of the grid-connected power system [39]. On the other hand, it is very complex to control the amplitude of three-phase currents under unbalanced grid faults, mainly because of the trend of simultaneously injecting both active and reactive power coupling positive/negative sequence grid voltage and current components. In such cases, the injection of the positive and negative sequence power inherently induces different amplitudes for the three-phase inverter output currents [40]. Therefore, the FRT control focus on the enhanced power quality and simplified peak current-limited control needs further research.

In addition, the presented current vector control technique for grid-connected inverter, which is based on the extended reactive power theory [41], enables us to assure the exchange of instantaneous active and reactive powers between a grid-connected inverter and the grid without power ripples. However, the method is derived from voltage/current vector and it is very complex.

In this paper, a modified instantaneous power control strategy based on phase compensation is proposed. The method focused on the reference currents algorithm. And the main demands laid on the grid-connected converter with harmonic-free currents, limited peak current magnitudes, and no fluctuations in demanded active and reactive powers under unbalanced grid voltage conditions, may be fulfilled together, contrary to the some references [11]-[13], [39], where an appropriate tradeoff must be usually considered.

In addition, the following features can be expected with the proposed method.

1) The computational perturbations of active and reactive power can be eliminated by the modified instantaneous power estimation at the same time without the expense of inverter current distortions.

2) The proposed method improved the power quality of the three-phase three-wire grid-connected power inverter under unbalanced grid voltage.

3) The proposed control methods are still acceptable under unbalanced grid voltage with some harmonics. It is easy to implement a current limitation function, which is beneficial for the reliable operations of the grid-connected system.

Finally, the experimental tests are carried out with the laboratory platform based dSPACE-DS1007 system. The experimental results are closely matching the theoretical analysis and expectations.

II. WORKING PRINCIPLE AND CONTROL STRATEGY

The structure of the grid-connected power electronic system under study is shown in Fig. 1. There is a three-phase three-wire inverter connected to the grid through an LCL-filter. In this study, it is assumed that a dc source is connected to the dc link of the inverter (such as a rectifier in wind plant control or a dc/dc converter in PV application), therefore, the dynamics from the dc link is not studied in this paper. The grid characteristics can be determined by the Short Circuit Ratio (SCR) parameters of the system [42].

The grid voltage sags fault can be expanded to symmetrical sags (type A) and asymmetrical sags (types B to G). However, the type C of unbalanced grid fault is the most common voltage sags in practice [10], where there is a phase shift in the faulty voltages.

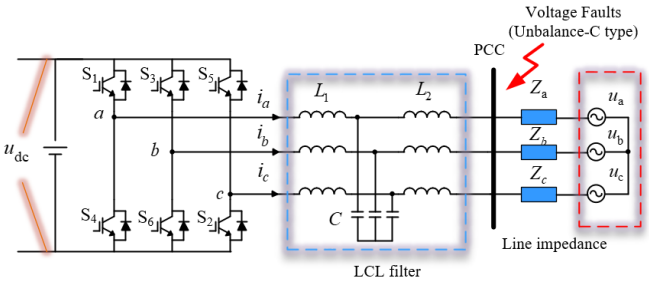

Fig. 1. Grid-connected inverter with an LCL filter under unbalanced grid voltage faults

A. Inherent reason for current harmonics and power oscillation for the conventional FRT solutions

For the convenience of analysis, the three-phase grid voltage can be expressed as follows

$$\begin{bmatrix} u_a \\ u_b \\ u_c \end{bmatrix} = \begin{bmatrix} U^+\sin(\omega t+\theta_p)+U^-\sin(\omega t+\theta_n) \\ U^+\sin(\omega t+\theta_p-120^\circ)+U^-\sin(\omega t+\theta_n+120^\circ) \\ U^+\sin(\omega t+\theta_p+120^\circ)+U^-\sin(\omega t+\theta_n-120^\circ) \end{bmatrix} \quad (1)$$

where θ_p ,θ_n, U^+, U^-, and ω represents the positive and negative sequence phase angle, voltage amplitude and angular frequency respectively.

With the Clarke transformation, the equation (1) can be expressed in the stationary frame as follows

$$\begin{cases} \begin{bmatrix} u_\alpha \\ u_\beta \end{bmatrix} = \frac{2}{3}\begin{bmatrix} 1 & -\frac{1}{2} & -\frac{1}{2} \\ 0 & \frac{\sqrt{3}}{2} & -\frac{\sqrt{3}}{2} \end{bmatrix}\begin{bmatrix} u_a \\ u_b \\ u_c \end{bmatrix} = \begin{bmatrix} u_\alpha^+ + u_\alpha^- \\ u_\beta^+ + u_\beta^- \end{bmatrix} \\ \begin{bmatrix} u_\alpha^+ \\ u_\beta^+ \end{bmatrix} = \begin{bmatrix} U^+\sin(\omega t+\theta_p) \\ -U^+\cos(\omega t+\theta_p) \end{bmatrix} \quad \begin{bmatrix} u_\alpha^- \\ u_\beta^- \end{bmatrix} = \begin{bmatrix} U^-\sin(\omega t+\theta_n) \\ U^-\cos(\omega t+\theta_n) \end{bmatrix} \end{cases} \quad (2)$$

According to the instantaneous power theory [6], the instantaneous active/reactive power can be described as

$$\begin{bmatrix} p \\ q \end{bmatrix} = \frac{3}{2}\begin{bmatrix} u_\alpha & u_\beta \\ u_\beta & -u_\alpha \end{bmatrix}\begin{bmatrix} i_\alpha \\ i_\beta \end{bmatrix} \quad (3)$$

This article has been accepted for publication in a future issue of this journal, but has not been fully edited. Content may change prior to final publication. Citation information: DOI 10.1109/JESTPE.2020.2984475, IEEE Journal of Emerging and Selected Topics in Power Electronics

where $i_{\alpha(p)}, i_{\beta(p)}, i_{\alpha(q)}$ and $i_{\beta(q)}$ represent the current active and reactive power components in the stationary frame respectively. Substituting (2) into (3), the active and reactive current components can be obtained as follows

$$\begin{cases} \begin{bmatrix} i_\alpha^* \\ i_\beta^* \end{bmatrix} = \frac{2}{3}\begin{bmatrix} u_\alpha & u_\beta \\ u_\beta & -u_\alpha \end{bmatrix}^{-1}\begin{bmatrix} P^* \\ Q^* \end{bmatrix} = \begin{bmatrix} i_{\alpha(p)}^* + i_{\alpha(q)}^* \\ i_{\beta(p)}^* + i_{\beta(q)}^* \end{bmatrix} \\ i_{a(p)}^* = \frac{2}{3}\dfrac{P^* u_\alpha}{(U^+)^2 + (U^-)^2 - 2U^+U^-\cos(2\omega t + \theta_p + \theta_n)} \\ i_{a(q)}^* = \frac{2}{3}\dfrac{Q^* u_\beta}{(U^+)^2 + (U^-)^2 - 2U^+U^-\cos(2\omega t + \theta_p + \theta_n)} \\ i_{\beta(p)}^* = \frac{2}{3}\dfrac{P^* u_\beta}{(U^+)^2 + (U^-)^2 - 2U^+U^-\cos(2\omega t + \theta_p + \theta_n)} \\ i_{\beta(q)}^* = -\frac{2}{3}\dfrac{Q^* u_\alpha}{(U^+)^2 + (U^-)^2 - 2U^+U^-\cos(2\omega t + \theta_p + \theta_n)} \end{cases} \quad (4)$$

where P^* and Q^* are the inverter output active and reactive power reference and detemined by the rated capacity of grid-connected inverter.

It should be noted that the inverter current components in (4) contain an amount of low-order harmonics because the denominator of current contains a double fundamental frequency fluctuation item as $2U^+U^-\cos(2\omega t + \theta_p + \theta_n)$.

Therefore, the reference [39] suggests that the inverter current harmonics can be eliminated on condition that $2U^+U^-\cos(2\omega t + \theta_p + \theta_n)$ in (4) is cancelled, which can be easily achieved with a notch filter of F (s) as shown in (5)

$$F(s) = \frac{s^2 + {\omega_n}^2}{s^2 + 2\xi\omega_c + {\omega_n}^2} \quad (5)$$

where ω_n is the notch frequency, and $\xi\omega_c$ is the cut-off frequency of the notch filter.

Thus, the current reference components in (4) will become sinusoidal and expressed in (6)

$$\begin{cases} i_{a(p)}^* = \frac{2}{3}\dfrac{P^* u_\alpha}{\left[(u_\alpha)^2 + (u_\beta)^2\right]F(\mathrm{s})} = \frac{2}{3}\dfrac{P^* u_\alpha}{(U^+)^2 + (U^-)^2} \\ i_{a(q)}^* = \frac{2}{3}\dfrac{Q^* u_\beta}{\left[(u_\alpha)^2 + (u_\beta)^2\right]F(\mathrm{s})} = \frac{2}{3}\dfrac{Q^* u_\beta}{(U^+)^2 + (U^-)^2} \\ i_{\beta(p)}^* = \frac{2}{3}\dfrac{P^* u_\beta}{\left[(u_\alpha)^2 + (u_\beta)^2\right]F(\mathrm{s})} = \frac{2}{3}\dfrac{P^* u_\beta}{(U^+)^2 + (U^-)^2} \\ i_{\beta(q)}^* = -\frac{2}{3}\dfrac{Q^* u_\alpha}{\left[(u_\alpha)^2 + (u_\beta)^2\right]F(\mathrm{s})} = -\frac{2}{3}\dfrac{Q^* u_\alpha}{(U^+)^2 + (U^-)^2} \end{cases} \quad (6)$$

Substituting (6) into (3), the instantaneous active and reactive power can be estimated as follows

$$\begin{aligned} p &= \frac{P^*}{(U^+)^2 + (U^-)^2}(u_\alpha^2 + u_\beta^2) \\ &= P^* - \overbrace{\frac{2P^*U^+U^-}{(U^+)^2 + (U^-)^2}\cos(2\omega t + \theta_p + \theta_n)}^{\tilde{P}} \end{aligned} \quad (7)$$

$$\begin{aligned} q &= \frac{Q^*}{(U^+)^2 + (U^-)^2}(u_\alpha^2 + u_\beta^2) \\ &= Q^* - \overbrace{\frac{2Q^*U^+U^-}{(U^+)^2 + (U^-)^2}\cos(2\omega t + \theta_p + \theta_n)}^{\tilde{Q}} \end{aligned} \quad (8)$$

It can be seen from equation (7) and (8), the sinusoidal current references can be achieved at the expense of active and reative power oscillations. Therefore, there is always a tradeoff between current harmonics and power oscillations for three-phase three-wire power systems from the viewpoint of the conventional instantaneous power theory.

B. Proposed current control strategy based on phase compensation

To solve this problem, the active and reactive power $\hat{p}$ and $\hat{q}$ can be expressed as a modified instantaneous power estimation formula as follows

$$\begin{bmatrix} \hat{p} \\ \hat{q} \end{bmatrix} = \frac{3}{2}\begin{bmatrix} u_\alpha & u_\beta \\ -u_\alpha F_d(s) & u_\beta F_d(s) \end{bmatrix}\begin{bmatrix} i_\alpha \\ i_\beta \end{bmatrix} = \frac{3}{2}\begin{bmatrix} u_\alpha & u_\beta \\ \hat{u}_\alpha & -\hat{u}_\beta \end{bmatrix}\begin{bmatrix} i_\alpha \\ i_\beta \end{bmatrix} \quad (9)$$

where $\hat{u}_\alpha$ and $\hat{u}_\beta$ represent the grid voltage components based compensated 135° and 45° phase angle, respectively.

It should be noted that the Band Pass Filter (BPF) F_d(s) here is a key piece of the control strategy. Therefore, its role and structure design should be discussed. The F_d(s) can achieve the beta voltage phase compensation of 45° as

$$F_d(s) = \frac{{\omega_d}^2}{s^2 + 2\xi\omega_c + {\omega_d}^2} \quad (10)$$

where ω_d can be set as the compensated phase voltage frequency, and $\xi\omega_c$ is the cut-off frequency of the filter. In addition, the compensated phase voltage frequency of the BPF is set as 50 Hz as a predefined value, which is the same with the grid voltage fundamental frequency. ξ is set to 1 for the good dynamic response as well as the filter performance. The alpha voltage phase compensation of 135° can be achieved by the -F_d(s).

With the same constant power control target, the active and reactive power references are P^* and Q^*. The inverter output current references are obtained from (9) and (10) as

$$\begin{cases} \begin{bmatrix} \hat{i}_\alpha^* \\ \hat{i}_\beta^* \end{bmatrix} = \frac{2}{3}\begin{bmatrix} u_\alpha & u_\beta \\ \hat{u}_\alpha & -\hat{u}_\beta \end{bmatrix}^{-1}\begin{bmatrix} P^* \\ Q^* \end{bmatrix} = \begin{bmatrix} \hat{i}_{\alpha(p)}^* + \hat{i}_{\alpha(q)}^* \\ \hat{i}_{\beta(p)}^* + \hat{i}_{\beta(q)}^* \end{bmatrix} \\ \hat{i}_{a(p)}^* = \frac{2}{3}\dfrac{P^*\hat{u}_\beta}{u_\alpha\hat{u}_\beta + \hat{u}_\alpha u_\beta} = \frac{2}{3}\dfrac{P^*\hat{u}_\beta}{(U^+)^2 - (U^-)^2} \\ \hat{i}_{a(q)}^* = \frac{2}{3}\dfrac{Q^* u_\beta}{u_\alpha\hat{u}_\beta + \hat{u}_\alpha u_\beta} = \frac{2}{3}\dfrac{Q^* u_\beta}{(U^+)^2 - (U^-)^2} \\ \hat{i}_{\beta(p)}^* = \frac{2}{3}\dfrac{P^*\hat{u}_\alpha}{u_\alpha\hat{u}_\beta + \hat{u}_\alpha u_\beta} = \frac{2}{3}\dfrac{P^*\hat{u}_\alpha}{(U^+)^2 - (U^-)^2} \\ \hat{i}_{\beta(q)}^* = -\frac{2}{3}\dfrac{Q^* u_\alpha}{u_\alpha\hat{u}_\beta + \hat{u}_\alpha u_\beta} = -\frac{2}{3}\dfrac{Q^* u_\alpha}{(U^+)^2 - (U^-)^2} \end{cases} \quad (11)$$

It should be noted that the denominator in (11) has become a constant component of $(U^+)^2 - (U^-)^2$ and without any notch filters. Therefore, the current references calculation will be reduced, and the inverter output currents

This article has been accepted for publication in a future issue of this journal, but has not been fully edited. Content may change prior to final publication. Citation information: DOI 10.1109/JESTPE.2020.2984475, IEEE Journal of Emerging and Selected Topics in Power Electronics

only consist of the fundamental positive and negative sequence grid voltage components, excluding the harmonic components. Therefore, the current quality is improved.

However, the peak value of current in (11) is obviously higher than the current components in (6) due to the negative sequence voltage component $U^{-} \neq 0$, which means there will be a higher overcurrent risk under unbalanced grid faults. Therefore, the next section will discuss the current limitation function of the proposed method.

C. Proposed control strategy equipped with currrent limitation function

In practice, the peak current is one of the most important factors to ensure the safe operation of grid-connected inverter under unbalanced grid fault. Therefore, the inverter should be equipped with a peak current limitation capacity. The limited peak current references are expressed as

$$\begin{cases} \begin{bmatrix} i_a^* \\ i_b^* \\ i_c^* \end{bmatrix} = \frac{I_{limit}}{I_{max}} \begin{bmatrix} \hat{i}_a^* \\ \hat{i}_b^* \\ \hat{i}_c^* \end{bmatrix} = \frac{I_{limit}}{I_{max}} \begin{bmatrix} \hat{i}_{\alpha(p)}^* + \hat{i}_{\alpha(q)}^* \\ \dfrac{-(\hat{i}_{\alpha(p)}^* + \hat{i}_{\alpha(q)}^*)}{2} + \dfrac{\sqrt{3}(\hat{i}_{\beta(p)}^* + \hat{i}_{\beta(q)}^*)}{2} \\ \dfrac{-(\hat{i}_{\alpha(p)}^* + \hat{i}_{\alpha(q)}^*)}{2} - \dfrac{\sqrt{3}(\hat{i}_{\beta(p)}^* + \hat{i}_{\beta(q)}^*)}{2} \end{bmatrix} \\ I_{max} = \max(\hat{i}_a^*, \hat{i}_b^*, \hat{i}_c^*) \end{cases} \quad (12)$$

where I_{limit} represents the limited value of the inverter current, I_{max} represents the maximum peak value in three phase currents.

It is clear that the current reference peak value in equation (12) will not go beyond the limited peak value of current during the unbalanced grid voltage fault.

In Fig. 2, eq. (9) instead of eq. (3) can be used for instantaneous active and reactive powers estimation. The voltage phase angles were compensated by F_d (s) and then send to current reference generations based on the instantaneous power theory. Thus, the active and reactive powers can be constant automatically.

Considering that the current harmonic amplitude reduces as its frequency increases, only the low-order current harmonics are regulated with the PR controller. Note that, for operating the PR controller under grid frequency variations, its resonant frequency should be updated with the grid frequency [39], and the detailed design of the PR controller can be found in [43]. The three-phase inverter currents are independently controlled by proportional resonant (PR) controllers with a single current-loop control.

However, it is still very complex to carry out the stability analysis under unbalanced and harmonic grid voltage. The main reason is that only the positive sequence model is considered under balanced grid without harmonics. However, for the unbalanced grid voltage with harmonics, not only the fundamental positive sequence model, but also fundamental negative sequence model, harmonics as well as the grid impedance all should be considered. The systematic and comprehensive modeling and stability analysis under unbalanced and harmonic grid voltage conditions still needs further research.

The current limitation function of (12) are working in three-phase frame, which is beneficial to the detection of the actual current peak values in real time. The detection of the current peak values can be easily estimated in a fast and accurate way as reported in [44-47].

Compared with the conventional peak current-limited control solutions, the proposed method is quite simple and does not need the information of the grid voltage unbalance factor, phase angle, and the extraction of positive and negative sequence voltage and/or current components. The proposed method only needs the detection of a maximum peak value in three-phase currents in real time. Therefore, the proposed method are easy to implement for industrial applications under both balanced and unbalanced grid voltage conditions.

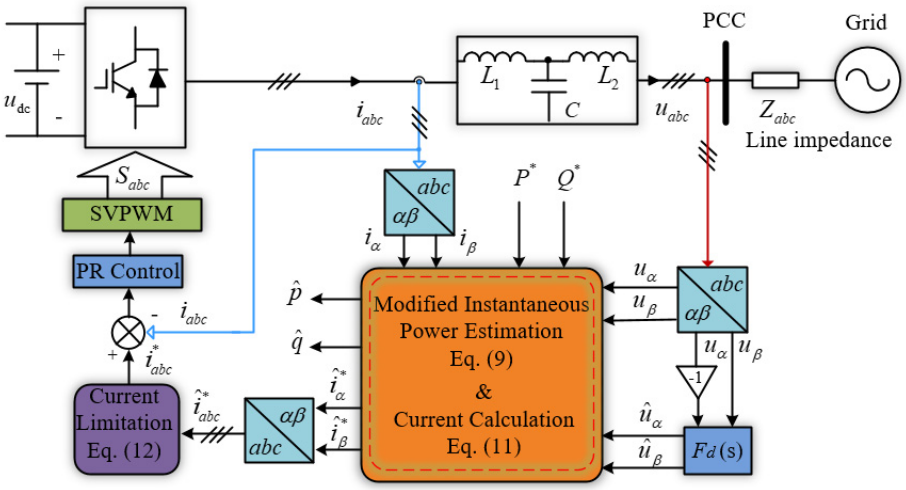

Fig. 2. Control diagram of proposed strategy with current limitation function

III. Simulation Results

To validate the proposed control method, the MATLAB/Simulink software was used. To emulate the C-type grid voltage fault, the Unbalance Factor (UF) of the grid voltage is set as 0.3, and there is a −137° and 137° angle in phase B and phase C, respectively. Assuming that the rated current of the power inverter is 5 A. The parameters of the simulated system are listed in Table I,

This article has been accepted for publication in a future issue of this journal, but has not been fully edited. Content may change prior to final publication. Citation information: DOI 10.1109/JESTPE.2020.2984475, IEEE Journal of Emerging and Selected Topics in Power Electronics

which are the same with the parameters of the experimental tests in the next section.

TABLE I. SYSTEM PARAMETERS

parameters	value	parameters	value
u_{dc}/V	720	u_a/V	300∠ 0°
u_b/V	145∠ −137°	u_c/V	145∠ 137°
U^+/V	230	U^-/V	70
P^*/kW	1.8	Q^*/kVar	1.35
L_1/mH	2	L_2 /mH	2
C/μF	10	UF	0.3
K_p	10.71	K_r	3587

The simulation results of the conventional and proposed control solutions under unbalanced grid voltage faults can be found in Fig.3, where the grid voltage faults are occurred at 0.2 seconds. At first, two conventional control methods (Solution I and Solution II) were presented to demonstrate the tradeoff between inverter current harmonics with its instantaneous powers oscillations, which means the current harmonics could be decreased at the expense of the larger fluctuations in both instantaneous active and reactive powers or vice versa. However, it should be noted that the power oscillations, large overcurrent and distortions under unbalanced voltage might lead to the failure of the FRT control during grid faults. On the other hand, the proposed control (Solution III) with voltage phase compensation can be used to improve the current quality while at the same time eliminate the instantaneous powers oscillations. However, the maximum peak current in solution III (8.5 A) is still larger than conventional solutions. Therefore, the proposed control methods should be equipped with current limitation function as demonstrated in solution IV and described in eq. (12).

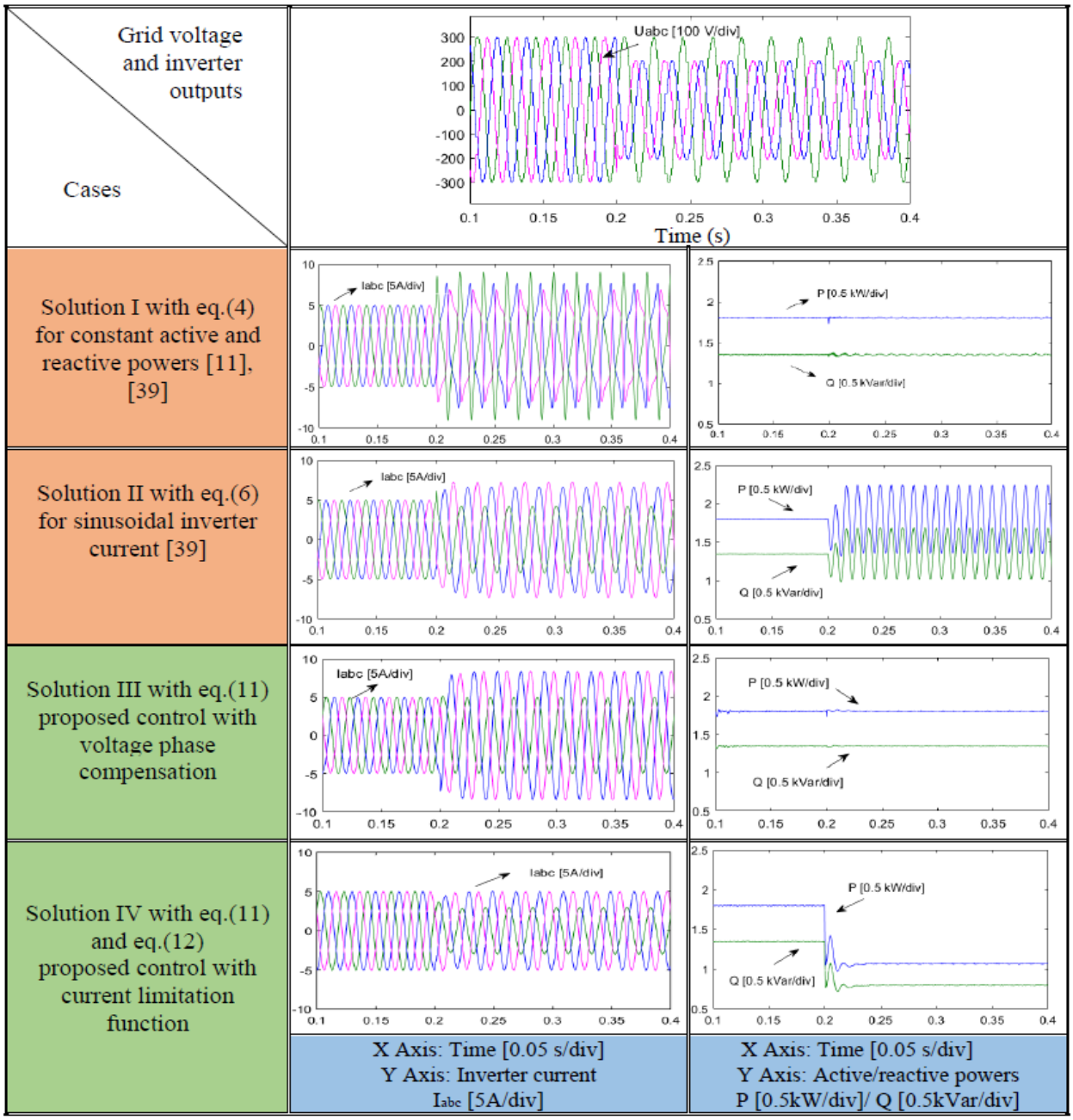

Fig.3. Simulation results of the conventional and proposed control solutions under unbalanced grid voltage fault

This article has been accepted for publication in a future issue of this journal, but has not been fully edited. Content may change prior to final publication. Citation information: DOI 10.1109/JESTPE.2020.2984475, IEEE Journal of Emerging and Selected Topics in Power Electronics

IV. Experimental Results

In addition, in order to further verify the effectiveness of the proposed control strategy, the experimental tests performed in the laboratory setup are shown in Fig. 4 (a) and Fig. 4 (b).

The grid-connected power system contains a three-phase three-wire 7.5 kW Danfoss inverter connected with an LCL filter. The dc link power is supplied by a Yaskawa D1000 active rectifier, which is controlled to be the desired value of 720 V. Chroma 61845 grid simulator is connected to support 300 V ac grid voltage, which will be specifically programmed to emulate the C-type unbalanced grid voltage fault during the experimental test. The experiments will divided into two cases, the first case focused on the unbalanced grid voltage without harmonics and the latter case is considered the unbalanced grid voltage contain with lower-order harmonics.

The proposed control solutions are implemented in the dSPACE-DS1007 system, where the switching pulses are generated via the digital waveform output board-DS5101. The inverter currents and the grid voltages are measured by an A/D-D/A multifunction board-DS2004. The sampling and switching frequencies are set as 10 kHz. The other parameters in the experiments are the same with the parameters of the simulated system.

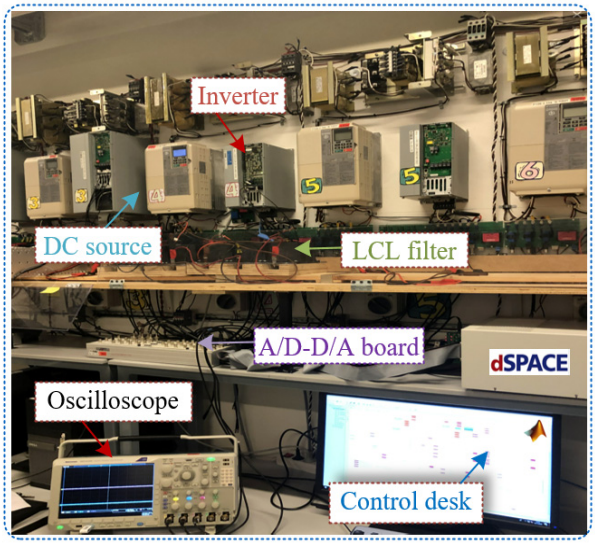

(a) Photo of the laboratory experimental setup

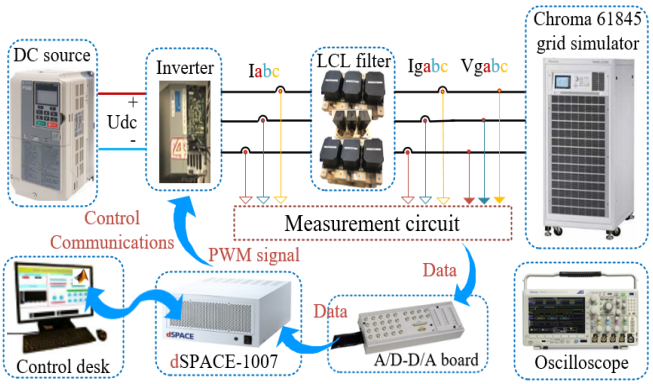

(b) Configuration of the grid-connected inverter system

Fig. 4. Laboratory platform based dSPACE-DS1007 system.

As shown in Fig. 5, a C-type unbalanced grid voltage fault occurred at 1.2 seconds. In this study case, the following will demonstrate the conventional FRT control solutions and the proposed control methods for comparison.

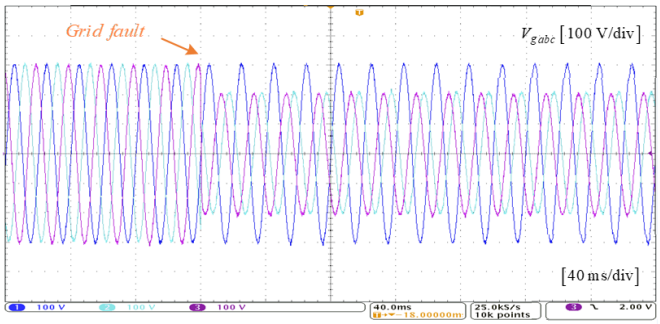

Fig. 5. C-type unbalance grid voltage fault without harmonics

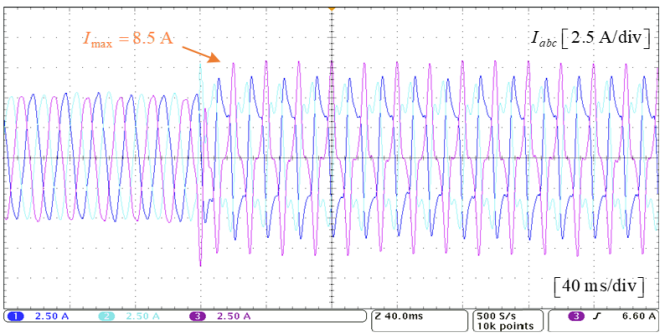

(a) Inverter output currents

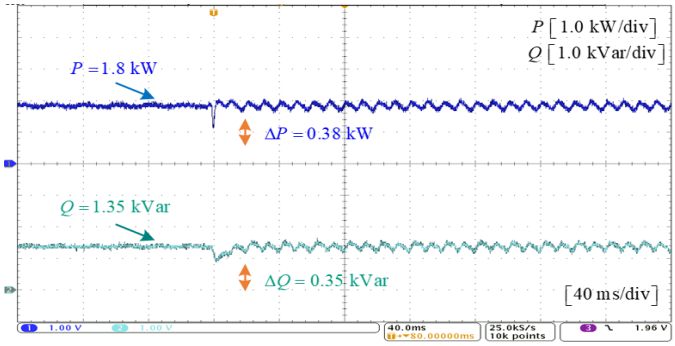

(b) Instantaneous active and reactive powers

Fig. 6. Conventional FRT control results (Solution I).

Fig. 6 shows the experimental results of conventional FRT control solution I with the current references based on (4), the active and reactive instantaneous power presents constant relatively during unbalanced grid voltage fault as shown in Fig. 6(b). There are small fluctuations in the active and reactive powers under unbalanced grid voltage cases. The fluctuations of the active and reactive power are 0.38 kW and 0.35 kVar, respectively, which are due to the phase shift errors in C-type unbalanced grid voltages.

However, it can be observed that the inverter output currents in Fig. 6(a) are highly distorted with an amount of low-order harmonics and the THD of currents are measured and it can even reach 31.84%, which is consistent with the theoretical analysis.

Fig. 7 presents the experimental results of conventional FRT control with current references based (6). As it can be seen in Fig. 7(a), the inverter output currents are controlled with normally sinusoidal waveforms at the expense of power fluctuations at the double fundamental frequency of the grid voltage (100 Hz) as shown in Fig. 7(b), and the instantaneous active and reactive power fluctuations are about 1.0 kW and 0.75 kVar, respectively.

This article has been accepted for publication in a future issue of this journal, but has not been fully edited. Content may change prior to final publication. Citation information: DOI 10.1109/JESTPE.2020.2984475, IEEE Journal of Emerging and Selected Topics in Power Electronics

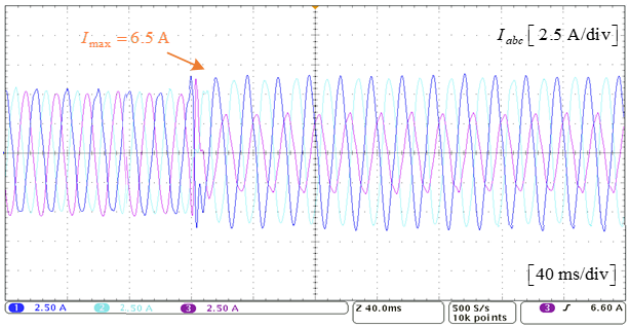

(a) Inverter output currents

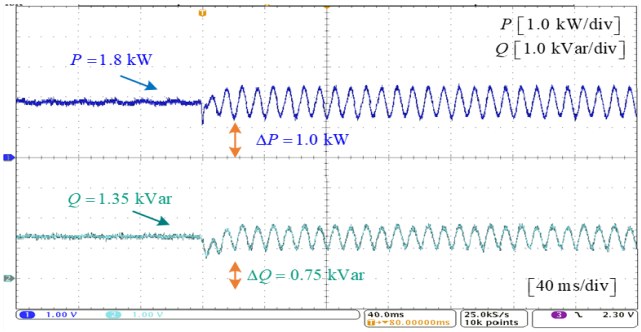

(b) Instantaneous active and reactive powers

Fig. 7. Conventional FRT control results (Solution II).

Besides, the experimental results are on good agreement with the theoretical analysis. It is evident that there is a tradeoff between inverter current harmonics and instantaneous power fluctuations for three-phase three-wire grid-connected inverter systems.

Accordingly, the lower harmonics in currents will lead to larger fluctuations in both active and reactive instantaneous powers. Therefore, the control target of pure sinusoidal waveforms of inverter currents and constant power estimation seems could not be achieved at the same time under unbalanced voltages from the conventional FRT solutions.

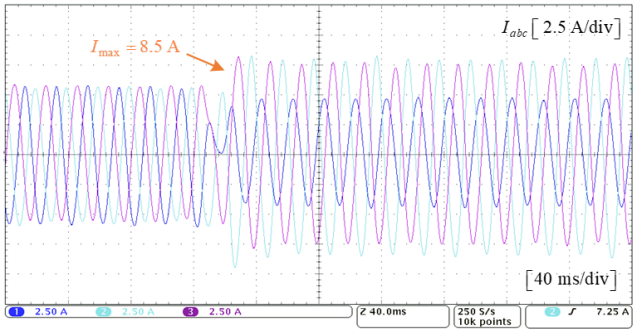

(a) Inverter output currents

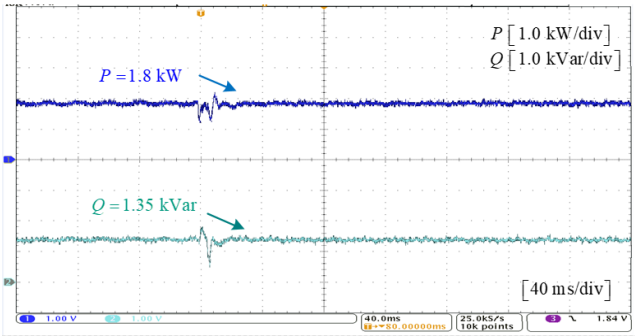

(b) Instantaneous active and reactive powers

Fig. 8. Proposed FRT control based on phase compensation results without a current limitation function (Solution III).

Fig. 8 shows the experimental results of the proposed control strategy based on (11) without current limitation function. It can be observed that the inverter output current harmonics can be greatly reduced and the active and reactive power can be estimated accurately at the same time due to the 45° and 135° phase angle compensation in alpha and beta voltage eliminating the fluctuant item in the denominator of the proposed current references in (11).

However, it is should be noted that the system experiences excessive overcurrent. The maximum peak value of the phase current is 8.5 A in Fig. 8(a), which is a higher than experimental results of conventional FRT solutions under unbalanced grid voltage, e.g. I_{max} = 7.5 A, shown in Fig. 7(a), and this may lead to a higher failure risk of FRT control under unbalanced grid faults. Therefore, it is necessary to equipped with current limitation function for the proposed control method.

Furthermore, Fig. 9 shows the experimental results of the inverter equipped with peak current-limited capacity based on the proposed method, and it can be seen from Fig.9(a) that the grid-connected inverter current can be well controlled within a limited range of 5A, which avoids the overcurrent risk compared with other control solutions during the grid faults. In Fig. 9(b), the instantaneous active and reactive power keeps constant and with a good dynamic performance, and the active and reactive power are decreased from 1.8kW to 1.0 kW and 1.35 kVar to 0.85 kVar, respectively, when the currents are limited.

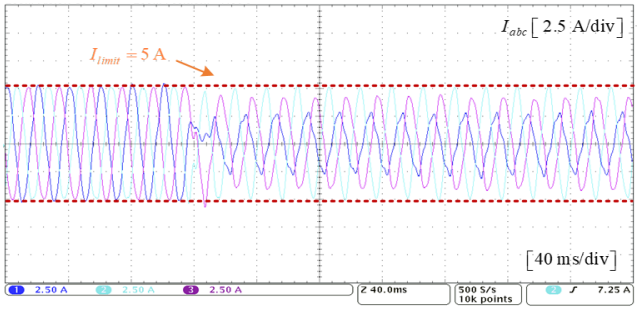

(a) Inverter output currents

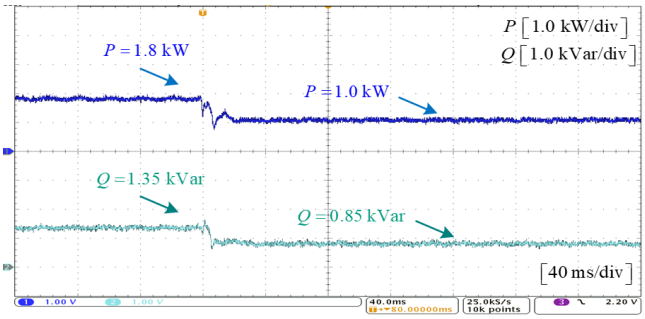

(b) Instantaneous active and reactive powers

Fig. 9. Proposed FRT control with a current limitation function results (Solution IV).

In order to further test and verify the effectiveness of the proposed control strategy under unbalanced grid voltage with harmonics. The experimental studies are carried out based on the above solutions. It is assumed that an unbalanced grid voltage mainly contains the low-order harmonics (eg. 4% of 5th harmonic, 3% of 7th harmonic and the THD of voltage is 5%) as shown in Fig. 10.

This article has been accepted for publication in a future issue of this journal, but has not been fully edited. Content may change prior to final publication. Citation information: DOI 10.1109/JESTPE.2020.2984475, IEEE Journal of Emerging and Selected Topics in Power Electronics

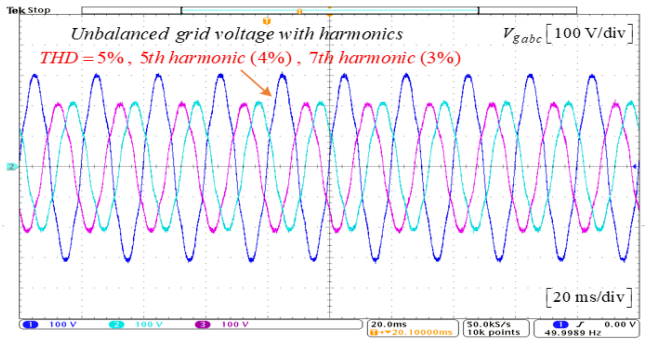

Fig. 10. Unbalanced grid voltage with harmonics.

Fig. 11 and Fig. 12 show the experimental results of conventional solution I and II under unbalanced grid voltage with 5th and 7th harmonics. It can be observed that the inverter current is more highly distorted, and the active and reactive power ripples are significantly increased due to the product function of the additional grid-connected inverter current harmonics and grid voltage harmonics, and even can be reached at 2.85 kV and 2.2 kVar, respectively, as shown in Fig. 12 (b).

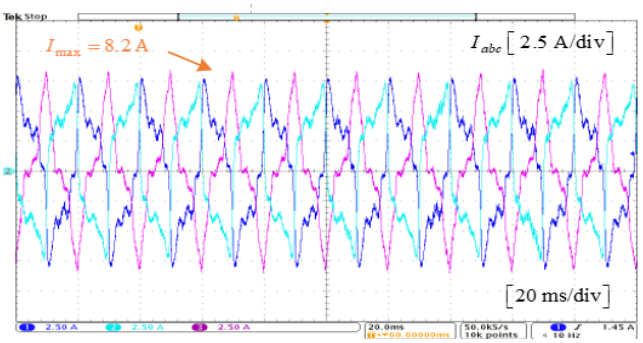

(a) Inverter output currents

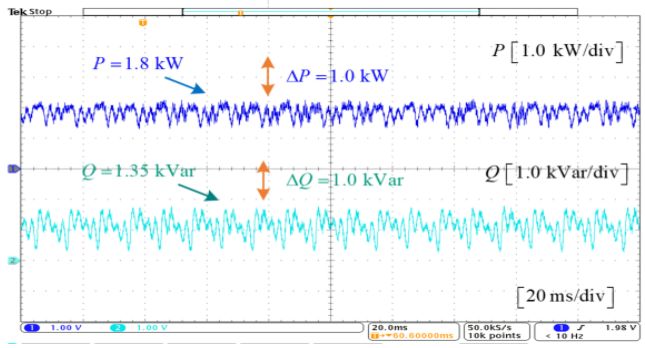

(b) Instantaneous active and reactive powers

Fig. 11. Solution I under unbalanced grid voltage with harmonics.

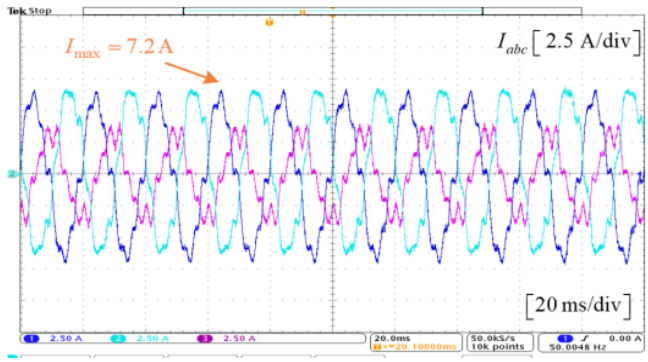

(a) Inverter output currents

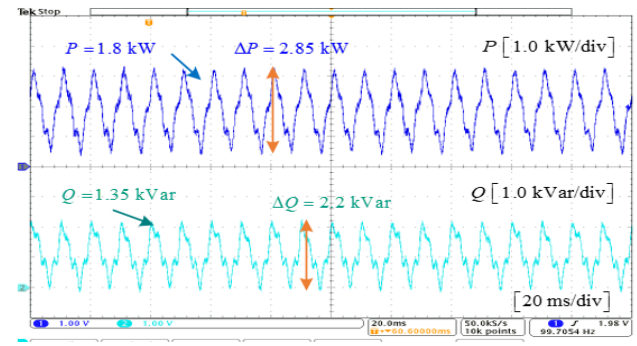

(b) Instantaneous active and reactive powers

Fig. 12. Solution II under unbalanced grid voltage with harmonics.

Fig. 13 and Fig. 14 show the experimental results of proposed solution III and IV under unbalanced and harmonic grid voltage. It can be seen the proposed strategy can still operates in a stable range, but the current harmonics are also increased as well as the active and reactive power ripples. Furthermore, the current peak value can be controlled within a limited range of 5A by solution IV as shown in Fig.14 (a). More performance comparison and quantified analysis can be found in Table.II.

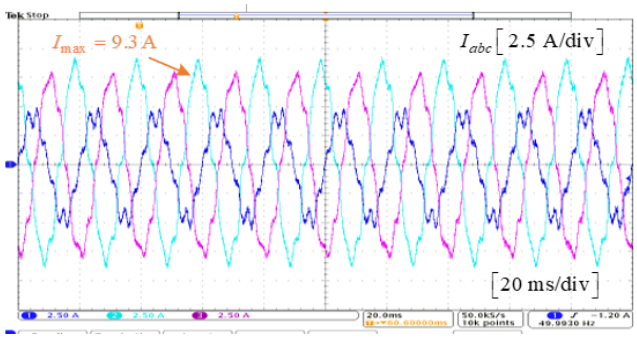

(a) Inverter output currents

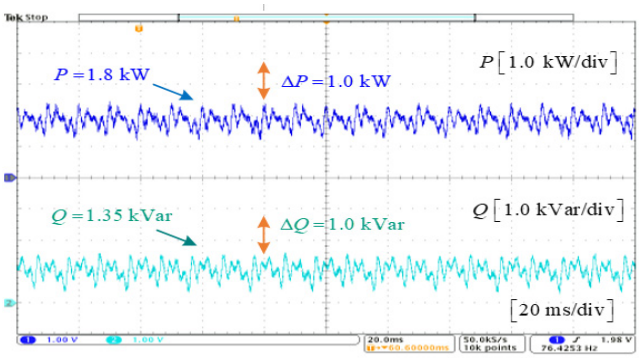

(b) Instantaneous active and reactive powers

Fig. 13. Solution III under unbalanced grid voltage with harmonics.

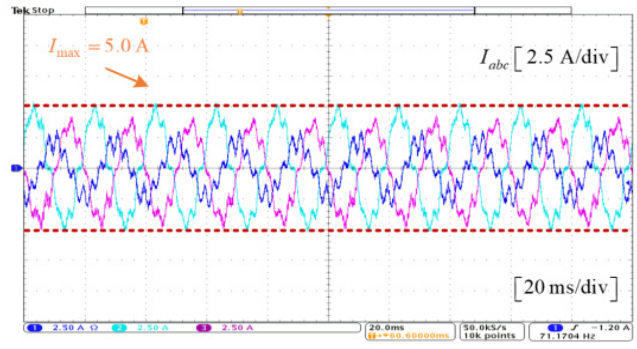

(a) Inverter output currents

This article has been accepted for publication in a future issue of this journal, but has not been fully edited. Content may change prior to final publication. Citation information: DOI 10.1109/JESTPE.2020.2984475, IEEE Journal of Emerging and Selected Topics in Power Electronics

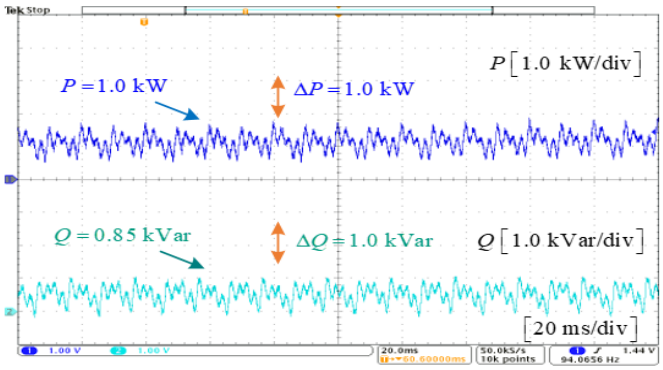

(b) Instantaneous active and reactive powers

Fig. 14. Solution IV under unbalanced grid voltage with harmonics.

TABLE.II. PERFORMANCE COMPARISON OF THE SOLUTIONS

	Unbalanced grid voltage without harmonics				Unbalanced grid voltage with harmonics			
	Current		Power		Current		Power	
	I_{max} [A]	THD_{max} [%]	ΔP_{max} [kW]	ΔQ_{max}[kVar]	I_{max} [A]	THD_{max}[%]	ΔP_{max} [kW]	ΔQ_{max}[kVar]
Solution I	8.4	31.64	0.38	0.35	8.2	34.57	1.02	1.02
Solution II	6.5	4.87	1.01	0.75	7.2	11.85	2.85	2.20
Solution III	8.5	4.06	0.01	0.01	9.3	6.51	1.00	1.00
Solution IV	5.0	6.94	0.01	0.01	5.0	12.91	1.00	1.00

V. CONCLUSION

In this paper, a modified instantaneous power control based on phase angle compensation and current limitation is proposed. For a fair comparison, the proposed methods have the same control structure with conventional solutions. All of the current references generation do not need any information from the grid voltage unbalance factor, phase angle, and extraction of positive and negative sequence voltage and/or current components. This reduces the computation burden since there is no Park transformation as well as PLLs.

In addition, the theoretical analysis and experimental verification of the proposed FRT control strategy are presented based on the three-phase three-wire inverter during C-type unbalanced grid faults. It is indicated that the proposed modified instantaneous power control (solution III) can enhance the inverter output current quality while mitigating the active and reactive power oscillations. However, the current harmonics are significantly increased as well as the active and reactive power ripples when the actual grid voltage harmonics are considered.

Furthermore, the peak current is one of the most important factors to ensure the safe operation of inverter to avoid overcurrent in practice. Therefore, the proposed solution IV is suggested to control the grid-connected inverter currents within a safe range to avoid the overcurrent risk effectively under the unbalanced grid voltage fault. The experimental results verify the effectiveness of the proposed solutions.

REFERENCES

[1] F. Blaabjerg, R. Teodorescu, M. Liserre, and A. V. Timbus, "Overview of control and grid synchronization for distributed power generation systems," *IEEE Trans. Ind. Electron*., vol. 53, no. 5, pp. 1398–1409, Oct. 2006.

[2] F. Blaabjerg, M. Liserre, and K. Ma, "Power electronics converters for wind turbine systems," *IEEE Trans. Ind. Appl.*, vol. 48, no. 2, pp. 708– 719, Mar./Apr. 2012.

[3] X. Wang, F. Blaabjerg, M. Liserre, et al. "An active damper for stabilizing power-electronics-based AC systems," *IEEE Trans. Power Electron.,* vol. 29, no. 7, pp. 3318–3329, Jul. 2014.

[4] C.-T. Lee, C.-W. Hsu, and P.-T. Cheng, "A low-voltage ride-through technique for grid-connected converters of distributed energy resources,"*IEEE Trans. Ind. Appl.,* vol. 47, no. 4, pp. 1821–1832, 2011.

[5] M. Johan, and S. De Haan. "Ridethrough of wind turbines with doubly-fed induction generator during a voltage dip," *IEEE Transactions on Energy Convers.*, vol. 20, no. 2, pp. 435-441. May. 2005.

[6] H. Akagi, E.H. Watanabe, and M. Aredes, "Instantaneous power theory and applications to power conditioning," Vol. 31. *John Wiley & Sons.* 2007.

[7] Y. Gui, X. Wang, and F. Blaabjerg,. "Vector current control derived from direct power control for grid-connected inverters, " *IEEE Trans. Power Electron.,* vol. 34, no. 9, pp. 9224–9235, Sep. 2019.

[8] Y. Gui, M. Li, J. Lu, S. Golestan, J. M. Guerrero, and J. C. Vasquez, "A voltage modulated DPC approach for three-phase PWM rectifier," *IEEE Trans. Ind. Electron.,* vol. 65, no. 10, pp. 7612–7619, Oct. 2018.

[9] H. Nian and L. Li, "Direct power control of doubly fed induction generator without phase-locked loop under harmonically distorted voltage conditions," *IEEE Trans. Power Electron.,* vol. 33, no. 7, pp. 5836–5846, Jul. 2018.

[10] W. Liu, X. Guo, and X. Zhao. et al. "Enhanced Power Quality and Minimized Peak Current Control in An Inverter based Microgrid

under Unbalanced Grid Faults," in *Proc. IEEE Energy Convers. Cong. Expo.*, 2016. pp.1-6.

[11] P. Rodriguez, A. V. Timbus, and R. Teodorescu, "Flexible active power control of distributed power generation systems during grid faults," *IEEE Trans .Ind. Electron.*, vol,54, no. 5, pp. 2583–2592, Aug. 2007.

[12] M. Reyes, P. Rodriguez, S. Vazquez, et al., "Enhanced decoupled double synchronous reference frame current controller for unbalanced grid-voltage conditions," *IEEE Trans. Power Electron.,* vol. 27, no. 9, pp. 3934–3943, Sep. 2012.

[13] F. Wang, J. L. Duarte, and M. A. M. Hendrix, "Pliant active and reactive power control for grid-interactive converters under unbalanced voltage dips, " *IEEE Trans. Power Electron.,* vol. 26, no. 5, pp. 1511–1521, Jun. 2011.

[14] A. Camacho, M. Castilla, J. Miret, et al. "Flexible Voltage Support Control for Three Phase Distributed Generation Inverters Under Grid Fault, " *IEEE Trans .Ind. Electron.*, vol. 60, no. 4, pp. 1429–1441, Jan. 2013.

[15] Y. Yang, F. Blaabjerg, and Z. Zou, "Benchmarking of grid fault modes in single-phase grid-connected photovoltaic systems," *IEEE Trans. Ind. Appl.,* vol. 49, no. 5, pp. 2167–2176, Sep./Oct. 2013.

[16] R. Teodorescu and F. Blaabjerg, "Flexible control of small wind turbines with grid failure detection operating in stand-alone and grid-connected mode," *IEEE Trans. Power Electron.,* vol. 19, no. 5, pp. 1323–1332, Sep. 2004.

[17] V. Soares, P. Verdelho, and G. D. Marques, "An instantaneous active and reactive current component method for active filters," *IEEE Trans. Power Electron.*, vol. 15, no. 4, pp. 660–669, Jul. 2000.

[18] X. Wang, L. Harnefors, and F. Blaabjerg, "Unified impedance model of grid-connected voltage-source converters," *IEEE Trans. Power Electron.*, vol. 33, no. 2, pp. 1775–1787, Feb. 2018.

[19] J. Miret, M. Castilla, A. Camacho, et al., "Control scheme for photovoltaic three-phase inverters to minimize peak currents during unbalanced grid-voltage sags," *IEEE Trans. Power Electron.*, vol. 27, no. 10, pp. 4262–4271. Mar. 2012.

[20] A. Camacho, M. Castilla, J. Miret, R. Guzman, and A. Borrell, "Reactive power control for distributed generation power plants to comply with voltage limits during grid faults," *IEEE Trans. Power Electron.*, vol. 29, no. 11, pp. 6224–6234, Jan. 2014.

[21] J. Hu, L. Shang, Y. He, and Z. Zhu, "Direct active and reactive power regulation of grid-connected DC/AC converters using sliding mode control approach," *IEEE Trans. Power Electron.,* vol. 26, no. 1, pp. 210–222, Jan. 2011.

[22] X. Guo, W. Liu, and Z. Lu, "Flexible power regulation and current-limited control of the grid-connected inverter under unbalanced grid voltage faults," *IEEE Trans. Ind. Electron.,* vol. 64, no. 9, pp. 7425–7432, Sep. 2017.

[23] K. Ma, W.J. Chen, M. Liserre, F. Blaabjerg, "Power controllability of a three-phase converter with an unbalanced AC source," *IEEE Trans. Power Electron*., vol. 30, no. 3, pp. 1591-1604, Mar. 2015.

[24] Z. Shuai, M. Xiao, J. Ge, and Z.J. Shen, "Overcurrent and Its Restraining Method of PQ Controlled Three-Phase Four-Wire Converter under Asymmetrical Grid Fault. " *IEEE J. Emerg. Sel. Topics Power Electron.*, vol. 7, no. 3, pp. 2057–2069, Dec. 2018.

[25] W. Zhao, X. Ruan, D. Yang, X. Chen, and L. Jia, "Neutral point voltage ripple suppression for a three-phase four-wire converter with an independently controlled neutral module," *IEEE Trans. Ind. Electron.,* vol. 64, no. 4, pp. 2608–2619, Apr. 2017.

[26] M. Malinowski, M. Jasinski, and M. P. Kazmierkowski, "Simple direct ´ power control of three-phase PWM rectifier using space-vector modulation (DPC-SVM)," *IEEE Trans. Ind. Electron.,* vol. 51, no. 2, pp. 447–454, Apr. 2004.

[27] T. Noguchi, H. Tomiki, S. Kondo, and I. Takahashi, "Direct power control of PWM converter without power-source voltage sensors," *IEEE Trans. Ind. Appl.,* vol. 34, no. 3, pp. 473–479, May/Jun. 1998.

[28] D. Zhi and L. Xu, "Direct power control of DFIG with constant switching frequency and improved transient performance," *IEEE Trans. Energy Convers.*, vol. 22, no. 1, pp. 110–118, Mar. 2007.

[29] X. Wang, and F. Blaabjerg, "Harmonic Stability in Power Electronic-Based Power Systems: Concept, Modeling, and Analysis," *IEEE Trans. Smart Grid,* vol. 10, no.3, pp. 2858-2870. May. 2019.

[30] E. Afshari, G. R. Moradi, R. Rahimi, et al., "Control strategy for three-phase grid-connected pv inverters enabling current limitation under unbalanced faults," *IEEE Trans. Ind. Electron.,* vol. 64, no. 11, pp. 8908–8918, Nov. 2017.

[31] L. Huang, H. Xin, Z. Wang, L. Zhang, K. Wu, and J. Hu, "Transient stability analysis and control design of droop-controlled voltage source converters considering current limitation," *IEEE Trans. Smart Grid,* vol. 10, no. 1, pp. 578–591, Jan 2019.

[32] K. Shi, W. Song, P. Xu, et al., "Low-voltage ridethrough control strategy for a virtual synchronous generator based on smooth switching," *IEEE Access*, vol. 6, pp. 2703–2711, 2018.

[33] Z. Shuai, W. Huang, C. Shen, J. Ge, and Z. J. Shen, "Characteristics and restraining method of fast transient inrush fault currents in synchronverters," *IEEE Trans. Ind. Electron.,* vol. 64, no. 9, pp. 7487–7497, Sep. 2017.

[34] A. D. Paquette and D. M. Divan, "Virtual impedance current limiting for inverters in microgrids with synchronous generators," *IEEE Trans. Ind. Appl.*, vol. 51, no. 2, pp. 1630–1638, March. 2015.

[35] S. F. Zarei, H. Mokhtari, M. A. Ghasemi, and F. Blaabjerg, "Reinforcing fault ride through capability of grid forming voltage source converters using an enhanced voltage control scheme," *IEEE Trans. Power Del.,* pp. 1–1, Jun. 2018.

[36] A. Gkountaras, S. Dieckerhoff, and T. Sezi, "Evaluation of current limiting methods for grid forming inverters in medium voltage microgrids," *Proc. IEEE Energy Convers. Cong. Expo*, 2015, pp. 1223–1230.

[37] W. Liu, T. Tomasz, C-L.Su, et al. "An evaluation method for voltage dips in shipboard microgrid under quasi-balanced and unbalanced voltage conditions," *IEEE Trans. Ind. Electron*., vol. 66, no. 10, pp. 7683-7693, Oct. 2019.

[38] W. Liu, T. Tomasz, and G. Mariusz, et al. "Power quality assessment in shipboard microgrids under unbalance and harmonic ac bus voltage, " *IEEE Trans. Ind. Appl.,* vol. 55 no. 1, pp. 7683-7693, Jan/Feb. 2019.

[39] X. Guo, W. Liu, X. Zhang, et al., "Flexible control strategy for grid-connected inverter under unbalanced grid faults without PLL, " *IEEE Trans. Power Electron.,* vol. 30, no. 4. pp. 1773-1778, Apr. 2015.

[40] A. Camacho, M. Castilla, J. Miret, et al. "Active and reactive power strategies with peak current limitation for distributed generation inverters during unbalanced grid faults," *IEEE Trans. Ind. Electron.,* vol. 62, no. 3, pp.1515-1525, Mar. 2015.

[41] V. Valouch, M. Bejvl, P. Šimek and J. Škramlík, "Power Control of Grid-Connected Converters Under Unbalanced Voltage Conditions," in *IEEE Transactions on Industrial Electronics*, vol. 62, no. 7, pp. 4241-4248, July 2015.

[42] M.G. Taul, X. Wang, P. Davari, and F. Blaabjerg, "Current Limiting Control with Enhanced Dynamics of Grid-Forming Converters during Fault Conditions," *IEEE J. Emerg. Sel. Topics Power Electron.*, 2019, in press. doi: 10.1109/JESTPE.2019.2931477.

[43] A. Vidal, F. D. Freijedo, A. G. Yepes, P. Fernandez-Comesana, J. Malvar, O. Lopez, and J. Doval-Gandoy, "Assessment and optimization of the transient response of proportional-resonant current controllers for distributed power generation systems," *IEEE Trans. Ind. Electron.,* vol. 60, no. 4, pp. 1367–1383, Apr. 2013.

[44] R.I. Bojoi, L.R., Limongi, D. Roiu, and A. Tenconi, "Enhanced power quality control strategy for single-phase inverters in distributed generation systems. " *IEEE Trans. Power Electron.*, vol. 26, no. 3, pp. 798-806, Mar. 2011.

[45] X. Du, Y Wu, S. Gu, H-M. Tai, P. Sun and Y. Ji, "Power oscillation analysis and control of three-phase grid-connected voltage source converters under unbalanced grid faults. " *IET Power Electronics*. vol. 9, no. 11, pp. 2162-2173, Sep. 2016.

[46] F. Nejabatkhah, Y. Li, K. Sun, and R. Zhang, "Active power oscillation cancelation with peak current sharing in parallel interfacing converters under unbalanced voltage," *IEEE Trans. Power Electron*, vol. 33, no.12, pp. 10200-10214, Dec. 2018.

[47] R.A.J. Amalorpavaraj, P. Kaliannan, S. Padmanaban, U. Subramaniam, and V.K. Ramachandaramurthy, " Improved fault ride through capability in DFIG based wind turbines using dynamic voltage restorer with combined feed-forward and feed-back control, " *IEEE Access*, vol. 5, pp. 20494-20503, Sep. 2017.

This article has been accepted for publication in a future issue of this journal, but has not been fully edited. Content may change prior to final publication. Citation information: DOI 10.1109/JESTPE.2020.2984475, IEEE Journal of Emerging and Selected Topics in Power Electronics

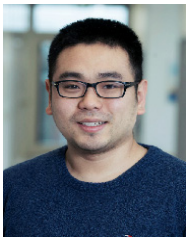

Wenzhao Liu (S'16-M'20) received the B.S. and M.S. degrees from Yanshan University, Qinhuangdao, China, in 2012 and 2015, and the Ph.D. degree from Aalborg University, Aalborg, Denmark, in Dec. 2018, all in electrical engineering. He has been a Ph.D. guest in Gdynia Maritime University, Gdynia, Poland, in 2017. Currently, he is a Postdoctoral Researcher in the Department of Energy Technology, Aalborg University, Aalborg, Denmark. His research interests include modeling, control, power quality and reliability assessment of power electronics based power systems and microgrids.

Frede Blaabjerg (S'86–M'88–SM'97–F'03) was with ABB-Scandia, Randers, Denmark, from 1987 to 1988. From 1988 to 1992, he got the PhD degree in Electrical Engineering at Aalborg University in 1995. He became an Assistant Professor in 1992, an Associate Professor in 1996, and a Full Professor of power electronics and drives in 1998. From 2017 he became a Villum Investigator. He is honoris causa at University Politehnica Timisoara (UPT), Romania and Tallinn Technical University (TTU) in Estonia. His current research interests include power electronics and its applications such as in wind turbines, PV systems, reliability, harmonics and adjustable speed drives. He has published more than 600 journal papers in the fields of power electronics and its applications. He is the co-author of four monographs and editor of ten books in power electronics and its applications. He has received 31 IEEE Prize Paper Awards, the IEEE PELS Distinguished Service Award in 2009, the EPE-PEMC Council Award in 2010, the IEEE William E. Newell Power Electronics Award 2014, the Villum Kann Rasmussen Research Award 2014 and the Global Energy Prize in 2019. He was the Editor-in-Chief of the IEEE TRANSACTIONS ON POWER ELECTRONICS from 2006 to 2012. He has been Distinguished Lecturer for the IEEE Power Electronics Society from 2005 to 2007 and for the IEEE Industry Applications Society from 2010 to 2011 as well as 2017 to 2018. In 2019-2020 he serves a President of IEEE Power Electronics Society. He is Vice-President of the Danish Academy of Technical Sciences too. He is nominated in 2014-2018 by Thomson Reuters to be between the most 250 cited researchers in Engineering in the world.

Dao Zhou (S'12-M'15-SM'19) received the B.S. from Beijing Jiaotong University, Beijing, China, in 2007, the M. S. from Zhejiang University, Hangzhou, China, in 2010, and the Ph.D. from Aalborg University, Aalborg, Denmark, in 2014, all in electrical engineering. Since 2014, he has been with Department of Energy Technology, Aalborg University, where currently he is an Assistant Professor. His research interests include modeling, control, and reliability of power electronics in renewable energy application. Dr. Zhou received the Renewable and Sustainable Energy Conversion Systems of the IEEE Industry Applications Society First Prize Paper Award in 2015, and Best Session Paper at Annual Conference of the IEEE Industrial Electronics Society (IECON) in Austria in 2013.

Shih-Feng Chou (S'09–M'17) He received the bachelor and master degrees in electrical engineering from National Tsing Hua University, Taiwan, in 2009 and 2011, respectively. After that, he became a firmware engineer in power electronics for renewable energy systems with Delta Electronics, Inc., Taoyuan, from 2012 to 2017. Now, he is a PhD student in the department of energy technology in Aalborg University, Denmark.His research focuses on the modeling of large-scale power electronics based power system.